

# PRESSURE-INDUCED DEPOLYMERIZATION OF SPINDLE MICROTUBULES

## II. Thermodynamics of In Vivo Spindle Assembly

E. D. SALMON

From the Marine Biological Laboratory, Woods Hole, Massachusetts 02543, and the Departments of Biology and Biomedical Electronic Engineering, University of Pennsylvania, Philadelphia, Pennsylvania 19174

### ABSTRACT

The present experiments were designed to test whether the simple equilibrium assembly model proposed by Inoué could predict variations in spindle microtubule assembly in response to changes in hydrostatic pressure as it does for changes in temperature. The results were also analyzed according to a model based on nucleated condensation polymerization since this recently appears to be the mechanism by which purified brain microtubules are assembled in vitro. Equilibrium birefringence (BR) of the meiotic metaphase-arrested spindle was measured in vivo as a function of hydrostatic pressure and temperature in *Chaetopterus* oocytes using a miniature microscope pressure chamber. Increasing pressure in steps to 3,000 psi at temperatures below 22°C did produce decreases in spindle equilibrium BR predictable directly from the simple equilibrium model of spindle assembly. Thermodynamic analysis of the pressure data yielded a value of  $\Delta \bar{V} \approx 400$  ml/mol of polymerizing unit. Theoretical curves based on the nucleated condensation model can also be made to fit the data, but semilog plots of the dependence of the equilibrium constant versus pressure and versus reciprocal temperature are biphasic, suggesting that either the size of the polymerizing unit changes or more than one equilibrium constant governs the assembly reaction. That the same value of  $\Delta \bar{V}$ , 90 ml/mol, was estimated from both the majority of the spindle BR data and data for the assembly of neural microtubules in vitro supports the possibility that spindle microtubules are assembled by a nucleated condensation mechanism.

The first paper of this series described how pressure (3,500–7,000 psi) caused the spindles of *Chaetopterus pergamentaceus* oocytes and several other types of cells to depolymerize rapidly and reversibly at normal physiological temperatures (47). The observed effects of pressure on the spindles were similar to reported effects of cooling

or of adding colchicine (25, 48). Qualitatively, the behavior of spindle microtubules in response to increased hydrostatic pressure was consistent with Inoué's concept of spindle assembly: that spindle fiber microtubules are in a labile "dynamic equilibrium" with a cellular pool of subunits (25).

From measurements of changes in the birefrin-

gence retardation (BR) of spindles in response to changes in temperature, Inoué and Morales (20, 21) formulated an equilibrium constant for the assembly of the spindle based on a simple equilibrium between monomer and polymer:

$$K(T) = \frac{(B)}{(A_o - B)}, \quad (1)$$

where (B) is the measured birefringence retardation (assumed to be proportional to the number of oriented assembled subunits in that region, or the concentration of polymer) and  $A_o$  is the upper limit of birefringence retardation (assumed to be proportional to the total amount of material in that region that is capable of being incorporated into microtubules, or to the concentration of monomer). Thermodynamic (van't Hoff) analysis of the temperature-BR data produced a linear relationship between  $\ln K$  and  $1/T^\circ K$ , and yielded large positive values of enthalpy ( $\Delta H = 28.4$  kcal/mol) and entropy ( $\Delta S = 101.0$  eu) of association. The large positive values of  $\Delta H$  and  $\Delta S$  were thought to be due to the dissociation or "melting" of constricted bound water away from the subunits during association (25, 31), a process also thought to be responsible for the large positive volume increase characteristic of in vitro self-assembly systems such as actin (1, 42) and tobacco mosaic virus (TMV) protein (37, 56). According to the model, the standard free energy of polymerization of the spindle ( $\Delta G^\circ$ ) was less than  $-1$  kcal/mol at normal physiological temperature ( $\approx 20^\circ C$ ), consistent with the characteristic lability of spindle fibers.

Numerous investigations have supported the assumptions of Inoué's assembly hypothesis. Changes in the number and distribution of spindle microtubules have been positively correlated with changes in the magnitude and distribution of spindle BR (17, 25, 26, 35, 39, 45). The microtubules in the central spindle lie essentially parallel to one another, thus producing the spindle's birefringence. Since the specific relationship between the number of microtubules in a spindle cross section and the magnitude of BR at that point is accurately described by Wiener's equation (40, 51), measurements of spindle BR are good indicators of the assembly of spindle fiber microtubules. Also, as a result of experiments by Stephens (54) which demonstrated that the amount of tubulin extracted from isolated spindles was proportional to the BR in vivo, measurements of spindle BR can be considered proportional to

the concentration of polymerized tubulin in the spindle region. Since spindle assembly is independent of immediate protein synthesis (25, 57), there must be a presynthesized pool of tubulin subunits from which the spindle fiber microtubules can be polymerized ( $A_o$  in equation [1]) (43, 60). Purified solutions of brain tubulin can stabilize and augment the size and BR of isolated spindles, thus documenting an equilibrium between spindle microtubules and a tubulin pool (5, 22, 44). Although the amount of tubulin in a cell far exceeds the requirements of the spindle (7, 43), it seems that the pool of tubulin actually available for spindle assembly is more limited. In one case, the size of the spindle pool could be controlled experimentally by changing the temperature during prophase (54).

Although numerous experiments have shown that Inoué's model can quantitatively account for changes in equilibrium spindle assembly (as measured by BR) induced by changes in temperature (5, 12, 50, 55), the model should also account for changes induced by hydrostatic pressure. The experiments reported in this paper were designed to examine the variation in equilibrium BR with pressure, at different constant temperatures, in the meiotic spindle of *Chaetopterus* oocytes, since this was the kind of spindle originally studied by Inoué. Because the animals used in these experiments were obtained from much deeper water than those studied previously by Inoué (20), the dependence of equilibrium spindle BR and the apparent pool size,  $A_o$ , on temperature was re-examined. The dependence of the metaphase equilibrium spindle BR upon pressure and temperature was then analyzed according to the Inoué simple equilibrium model to see how well the model could describe the data. For comparison, the results were also analyzed according to a model of microtubule assembly based on nucleated condensation polymerization, since this appears to be the mechanism by which labile brain microtubules assemble in the test tube (13, 41).<sup>1</sup>

## MATERIALS AND METHODS

### *Experimental Material and Apparatus*

Oocytes from the annelid *Chaetopterus pergamentaceus* were used in all of the present experiments. Source and care of the animals, collection of gametes, normal behavior of the spindle, and cell preparation are de-

<sup>1</sup>Salmon, E. D. 1975. Pressure-induced depolymerization of brain microtubules in vitro. *Science (Wash. D.C.)*. In press.

scribed in detail elsewhere (47). The pressure chamber, polarized light microscope system, and methods for generating pressure, controlling temperature, measuring BR, and photography have also been described elsewhere (47, 49).

### *Experimental Protocol*

At the beginning of each experiment, approximately 20–40 eggs, or egg fragments cleared of yolk, were mounted onto the center of the lower window in the pressure chamber, and the chamber was filled with filtered sea-water at  $\approx 22^\circ\text{C}$  and then sealed (49). The cell nearest to the center of the chamber window having a spindle attached to the cell surface and oriented in the plane of the window was usually chosen for observation. The spindle BR at  $22^\circ\text{C}$  was then measured and the spindle photographed. The temperature was kept constant ( $\pm 0.3^\circ\text{C}$ ) for most of the experiments at  $22^\circ\text{C}$  (22 cells), but the temperature was shifted to  $17.5^\circ\text{C}$  (14 cells) or  $14.5^\circ\text{C}$  (7 cells) in other experiments.

The basic procedure for a single experiment consisted of systematically raising the chamber pressure, usually in steps of 500 psi. At each step the pressure was held constant for approximately 6–7 min to allow sufficient time for the spindle to reach its new equilibrium state (47). At each equilibrium the BR was measured five to eight times, to be averaged later, and the spindle was photographed. When pressure produced such weak BR that accurate measurement was too difficult, the pressure was released. At atmospheric pressure the spindle recovered completely in 20–25 min (47). The total time under pressure was kept within 35–40 min. Often, this procedure was repeated several times on the same cell.

The basic procedure was also varied as follows. In several experiments different size pressure steps were used (300–2,000 psi). Occasionally, the pressure was systematically decreased in discrete steps back to atmospheric pressure after the spindle had completely disappeared. Although most of the experiments were performed on flattened eggs, spindles in several stratified eggs and 0.25-vol egg fragments were examined at  $22^\circ\text{C}$ . Also, to check the long-term stability and reversibility of the spindle equilibrium under pressure, one group of cells was held at 1,900 psi, and another group at 3,000 psi for approximately 2.5 h while changes in spindle BR and size were monitored. In several experiments (six cells) the pressure was kept at atmospheric level and the chamber temperature systematically varied between  $35^\circ\text{C}$  and  $5^\circ\text{C}$  to re-examine the dependence of spindle equilibrium BR on temperature.

At the end of several of the experiments, the cells were fertilized by replacing the chamber seawater with seawater containing a dilute suspension of sperm. The cells divided normally, and only rarely did the pressure treatment appear to have induced any detrimental effect on development up to the 16-cell stage.

## RESULTS

Increased pressure decreased the spindle BR and size to new equilibrium values that remained constant for a minimum of 35–40 min (Fig. 1). Spindles reached their new equilibrium BR and size rapidly: within 1 min for BR and within 6 min for size. Spindles recovered completely after being returned to atmospheric pressure, even when pressures twice that required to cause complete spindle disappearance were held for 30 min. The BR increased rapidly, but recovery of the original size normally required 15–20 min.

Quantitatively, increased pressure produced predictable decreases in equilibrium spindle BR (Fig. 2). Although most of the data in Fig. 2 were obtained from spindles in flattened cells with pressure increased in steps of 500 psi, the magnitude of BR was largely independent of experimental factors other than pressure and temperature. Spindles in stratified eggs or yolk-free 0.25-vol egg fragments responded exactly as did the spindles in whole nonstratified eggs. At  $22^\circ\text{C}$ , experiments using equilibrium pressure steps of 1,000 or 2,000 psi produced essentially the same response as when pressure was raised to an equivalent magnitude with smaller equilibrium steps. After application of pressures that almost abolished the spindle (e.g., 2,500 psi at  $22^\circ\text{C}$ ), returning to a lower pressure produced a BR similar to that obtained by going directly from atmospheric pressure, provided the total time under pressure was less than 35–40 min.

The equilibrium spindle length decreased proportionally with increasing pressure (Fig. 3). As with changes in spindle BR with pressure, changes in length were independent of the size of the pressure step or whether the spindle was in a whole cell or cell fragment.

Preliminary evidence suggests that the microtubules of the spindle adapt to moderate pressures that are held longer than 35–40 min at  $22^\circ\text{C}$ , particularly pressures that cause almost complete spindle depolymerization (Figs. 4, 5). After about 35 min both the BR and the size of the spindle began to increase slowly; the spindle appeared almost normal in size and shape after about 1.5 h, but had only two-thirds the original BR. A longer and more birefringent spindle than normal regrew after atmospheric pressure was restored. Also, additional aster structures appeared within the egg. After about 1 h the additional asters disappeared and the spindle returned to normal size and BR. These responses were typical of all 12 cells observed at about 2,000 psi. No spindles were

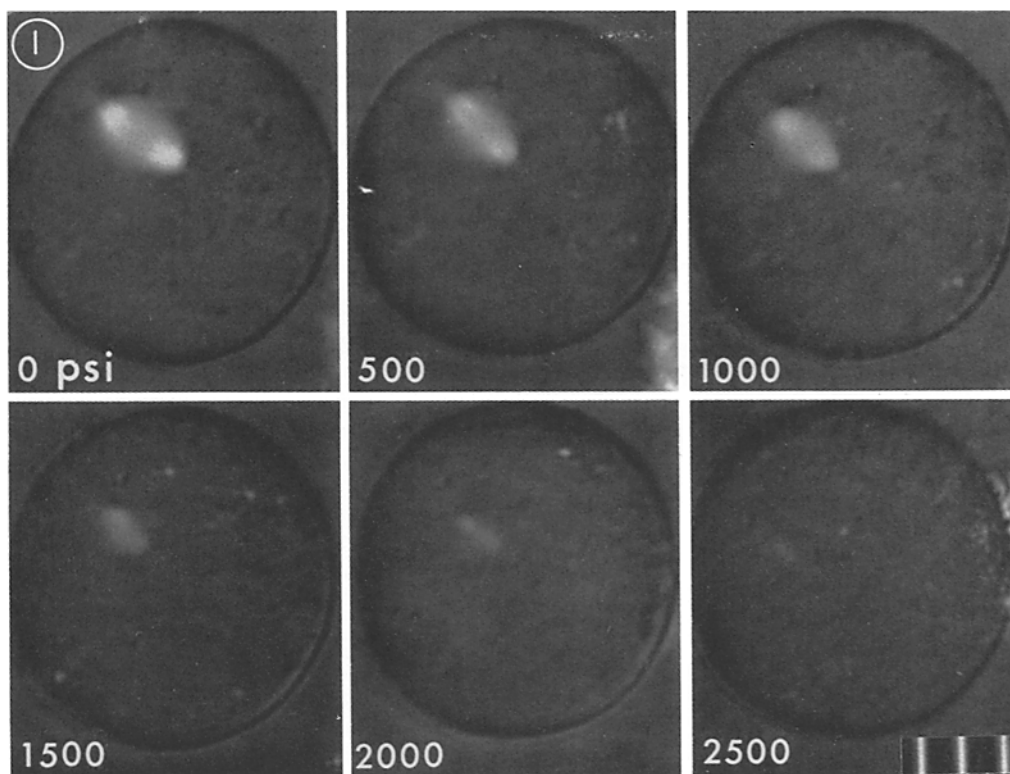


FIGURE 1 Changes in equilibrium spindle BR and size as a function of pressure for a spindle in a clear 0.25-vol fragment. The pressure was increased by 500 psi every 7 min. Photographs were taken 6 min after each pressure increment at which time the spindle had reached its new equilibrium. Spindle is slightly tilted and one pole is somewhat out of focus. Scale = 10  $\mu$ m spacing.

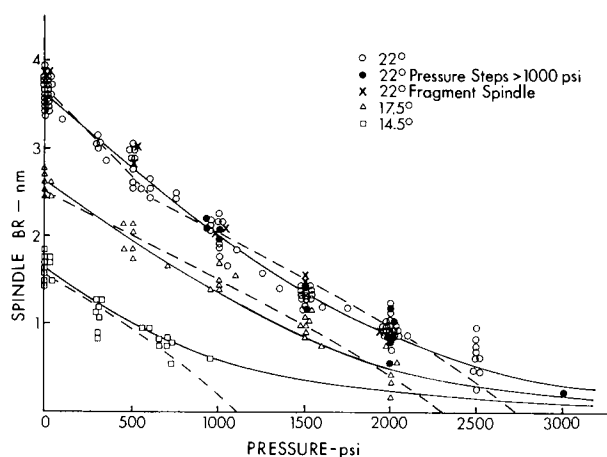


FIGURE 2 Equilibrium spindle BR as a function of pressure at constant temperatures of 22°C, 17.5°C, and 14.5°C. All data points are presented. Data include measurements on spindles in whole eggs and egg fragments as well as for both large and small pressure increments. Solid lines were derived from the Inoué simple equilibrium model and the dashed lines were derived from the nucleated condensation model as explained in the text.

observed in cells held at 3,000 psi for 2 h, but after pressure was released, spindles regrew to a size and BR larger than normal, similar to the response shown in Fig. 4. Because of this adaptive behavior,

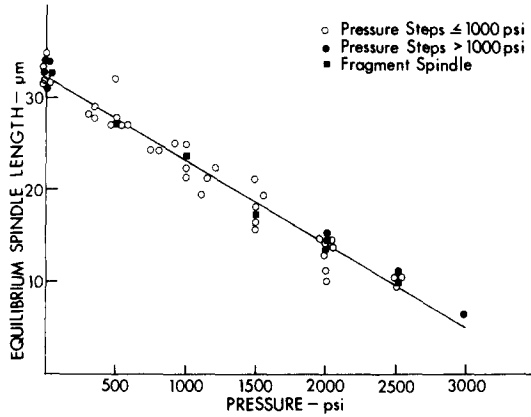


FIGURE 3 Equilibrium spindle pole-to-pole length as a function of pressure. The data were taken from photographs of spindles that had both poles clearly in focus during the experiments in Fig. 2. Confidence limits for each data point are about  $\pm 1 \mu\text{m}$ . The line having a slope of  $9.0 \pm 0.3 \mu\text{m}/1,000 \text{ psi}$  through the data points was fitted by the method of least squares.

all experiments for which equilibrium data are presented were conducted so that the total period of pressurization was less than 35–40 min.

The variation in equilibrium spindle BR with temperature is plotted in Fig. 6 with Inoué's data for comparison (20). In the present experiments, the changes in spindle BR with temperatures below  $23^\circ\text{C}$  were reversible and similar to the previous data. At temperatures above  $23^\circ\text{C}$ , however, instead of becoming larger and more birefringent as the temperature increased, the spindles decreased in both size and BR, becoming irreversibly depolymerized at temperatures above  $30^\circ\text{C}$ . Consequently, the pressure equilibrium studies described above were performed at temperatures of  $22^\circ\text{C}$  and lower. Changes in spindle BR with temperature were accompanied by similar changes in spindle length, but a quantitative analysis was not performed.

#### Data Analysis

Given Inoué's assumptions and the simple equilibrium model (equation [1]), the equilibrium constant of the assembly reaction, formed from the spindle BR data for the spindle arrested in metaphase, should be a function of temperature and

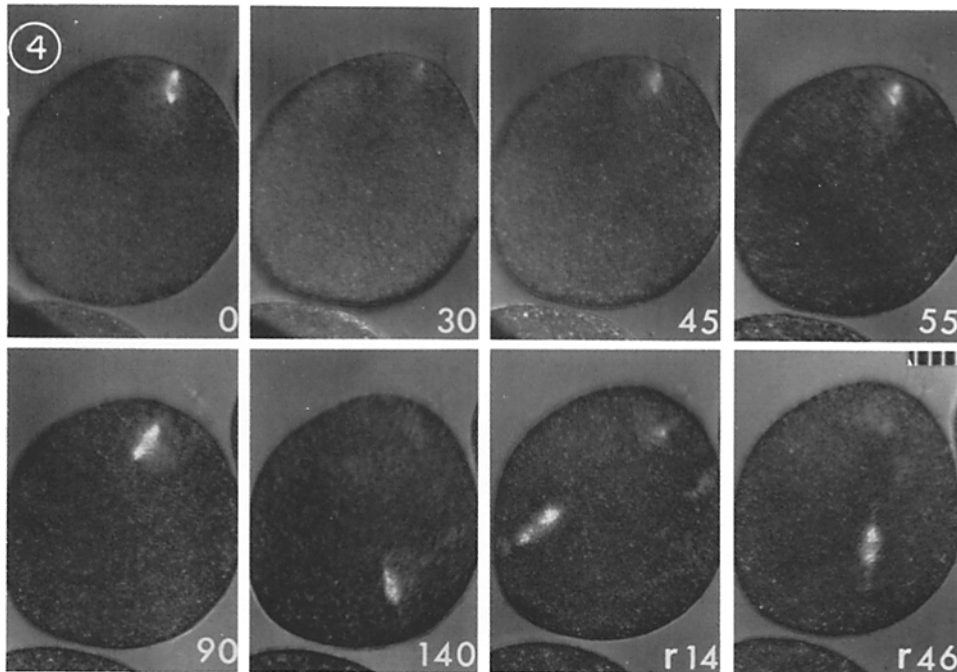


FIGURE 4 Adaptation of the spindle to long-term pressurization of 1,900 psi. Time in minutes is indicated on each print with the time set to zero at pressure application and again at pressure release (146 min after pressurization). Notice the migration of the spindle through the egg and the formation of additional aster structures after pressure release. Scale =  $10 \mu\text{m}$  spacing.

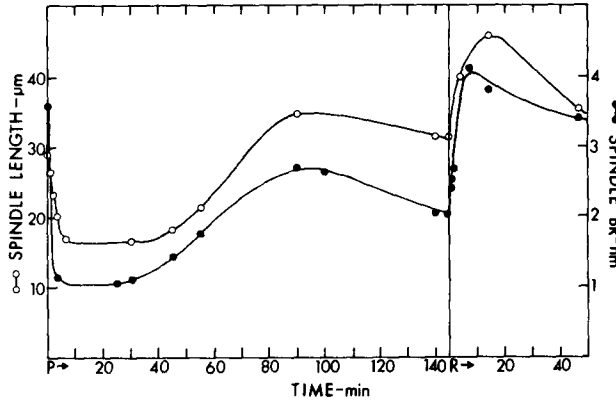


FIGURE 5 Spindle BR and pole-to-pole length changes resulting from pressure adaptation of the cell in Fig. 4. The dropping of the curves between 90 and 140 min may be due to long-term respiratory effects of cell crowding within the chamber.

pressure as (see Appendix):

$$K(T,P) = \frac{(B)}{(A_o - B)}$$

$$= \exp [-\Delta G_i^0/RT - (P - 14.7) \Delta \bar{V}/RT]. \quad (2)$$

$\Delta G_i^0$  is the change in standard Gibbs free energy at atmospheric pressure and  $\Delta \bar{V}$  the change in molar volume per subunit between the polymerized and unpolymerized state. Inoué's simple equilibrium model was based on the concept that subunits making up the spindle fibers are capable of participating in the equilibrium reaction (21).

A nucleated condensation polymerization process, however, whose equilibrium is independent of the amount of material in polymerized form, is thought to be responsible for polymerization of long fibers such as actin (1, 30, 42), and bacterial flagellin (14, 15), as well as microtubules in vitro (13, 41).<sup>1</sup> Polymerization and depolymerization occur only at the ends of the fibers and the net rate of microtubule polymerization is given by the relation (derived from Kasai, reference 30):

$$dB/dt = k_1 N_f (A_o - B) - k_2 N_f, \quad (3)$$

where, according to Inoué's assumptions,  $B$  represents the amount of polymerized subunit,  $(A_o - B)$  represents the unpolymerized tubulin concentration,  $N_f$  is the concentration of fiber ends, and  $k_1$  and  $k_2$  are the rate constants. At equilibrium  $dB/dt = 0$ , and the equilibrium constant will be given by:

$$K(T,P) = k_2/k_1 = N_f/(N_f)(A_o - B)$$

$$= 1/(A_o - B). \quad (4)$$

Since  $\Delta G_i^0$  is a function only of temperature, for either model a plot of log equilibrium constant as a function of pressure, at constant temperature, should be a linear function of pressure:

$$\ln K = -\Delta G_i^0/RT - (P - 14.7) \Delta \bar{V}/RT; \quad (5)$$

assuming a constant value of  $\Delta \bar{V}$  over the pressure and temperature ranges studied. The equilibrium constant for spindle assembly was calculated for the averages of the data points at each pressure in Fig. 1 according to both the Inoué simple equilibrium model (equation [2]) and the nucleated condensation model (equation [4]). The value  $A_o = 5.8$ , determined from the temperature analysis explained below, was used to calculate the equilibrium constants.

As seen in Fig. 7 a, the pressure dependence of  $\ln K$ , based on the simple equilibrium model, can be fitted by a family of straight lines (method of least squares) which have nearly identical slopes that yield estimates of the molar volume change of association (according to equation [2]) of  $\Delta \bar{V} = 394$  ml/mol for 22°C,  $\Delta \bar{V} = 387$  ml/mol for 17.5°C, and  $\Delta \bar{V} = 493$  ml/mol for 14.5°C. Since the tendency to underestimate spindle BR at low temperatures could account for the larger volume change at 14.5°C, it seems reasonable to conclude that, according to the simple equilibrium model, the volume change of polymerization remains constant at approximately 400 ml/mol over the temperature and pressure ranges studied. The data in Fig. 2 closely fit theoretical curves calculated from equation (2) using the value  $\Delta \bar{V} = 400$  ml/mol and intercepts of the least-square lines in Fig. 7 a.

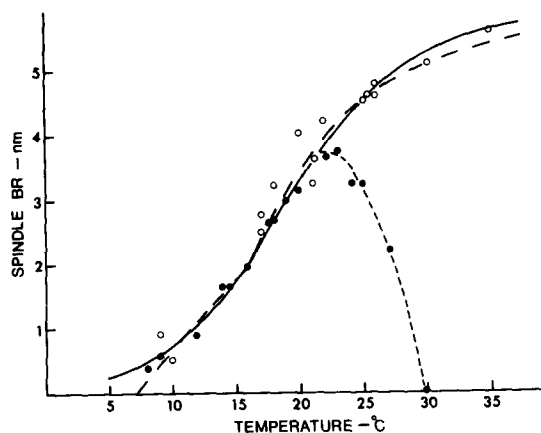


FIGURE 6 Spindle BR as a function of experimental temperature including data previously obtained by Inoué (20) (open circles) for comparison with the present experimental data (solid circles). For the present experiments each spindle BR value represents the average of three or more measurements on different spindles, with the exception of the points at 8°C and 9°C which represent single measurements. The maximum variation in values for a given temperature was  $\pm 0.35$  nm. In five cells studied, temperatures greater than 30°C produced complete, irreversible spindle depolymerization within about 10 min. The solid line was derived from the Inoué simple equilibrium model and the long-dashed line from the nucleated condensation polymerization model as described in the text. The short-dashed line was fitted by eye.

Fig. 7 *b* presents the analysis of the pressure data according to the nucleated condensation model (equation [4]). At 17.5°C and 14.5°C the data can be closely fitted by straight lines whose slopes yield the value  $\Delta \bar{V} = 87$  ml/mol for 17.5°C, and  $\Delta \bar{V} = 94$  ml/mol for 14.5°C. The data at 22°C are fitted, however, by two straight lines. For pressure below 650 psi the slope yields a value  $\Delta \bar{V} = 271$  ml/mol, and above 650 psi the slope yields a value  $\Delta \bar{V} = 90$  ml/mol. When modified in this manner, theoretical curves based on the nucleated condensation model (equation [4]) fit the spindle BR data in Fig. 2 almost as well as the simple equilibrium model.

Calculated from the simple equilibrium model,  $\ln K$  varies as a linear function of reciprocal temperature as seen from the van't Hoff analysis of both Inoué's data alone and a composite of Inoué's data and data from the present experiments below 23°C (Fig. 8 *a*). The value  $A_0 = 6.0$ , determined by Inoué (20), was used initially as the

estimate of the pool size for the van't Hoff analysis, then adjusted to 5.8 to give the best least squares fit of each data set to a straight line by statistical linear regression analysis ( $r = -0.978$  for Inoué's data,  $r = -0.982$  for the composite data). The variation in  $\ln K$  vs. reciprocal temperature at atmospheric pressure is given from equation (2) as:

$$\ln K = -\Delta G_1^0/RT \\ = -(\Delta H/R)(1/T) + \Delta S/R, \quad (6)$$

where  $\Delta H$  is the change in enthalpy and  $\Delta S$  the change in entropy per subunit in going from the unpolymerized to the polymerized state. The slopes of the least-squares lines yielded values of  $\Delta H = 34$  kcal/mol for Inoué's data and  $\Delta H = 36$  kcal/mol for the composite data. The intercepts yielded the values  $\Delta S = 117$  eu for Inoué's data alone and  $\Delta S = 124$  eu for the composite data. These thermodynamic parameters are somewhat larger than those previously reported by Inoué (20) ( $\Delta H = 28.4$  kcal/mol and  $\Delta S = 101.0$  eu), probably as a result of differences in the methods used to analyze the data. As previously found by Inoué (20), equal amounts of polymer and monomer ( $\Delta G_1^0 = 0$ ) appear to exist at a temperature of about 20°C.

When the equilibrium constant  $K$  is formulated according to the nucleated condensation model, the variation in  $\ln K$  with reciprocal temperature is not a simple linear function (Fig. 8 *b*). As with the pressure data at 22°C, the temperature data can be fitted by two straight lines. The slopes of these least-squares lines yield values of  $\Delta H = 22$  kcal/mol ( $T \geq 16^\circ\text{C}$ ) and  $\Delta H = 7.5$  kcal/mol ( $\leq 16^\circ\text{C}$ ). The value of  $\Delta S$  cannot be determined from the condensation model because the equilibrium constant is not dimensionless. The theoretical curves in Fig. 6 for a nucleated condensation model, calculated from the least-squares lines in Fig. 8 *a* and *b* using equations (2), (4), and (6), predict the temperature spindle BR data as well as the simple equilibrium model does.

Analyzing the data according to a model of linear condensation ( $K = (B)/(A_0 - B)^2$ ) produced curves, not shown, that fit the pressure and temperature data for the *Chaetopterus* spindles about as well as the simple equilibrium model fit the data, but yielded larger thermodynamic parameters (Table I). Although TMV protein is believed to be polymerized by a linear condensa-

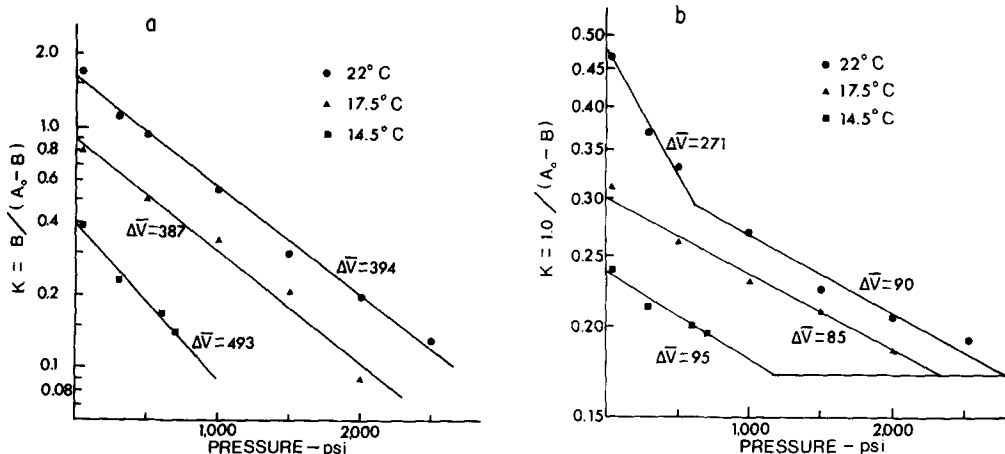


FIGURE 7 Dependence of the equilibrium constant on pressure. The equilibrium constant was found for the average value of the BR data points at each major experimental pressure in Fig. 2 according to: (a) the simple equilibrium model,  $K = (B)/(A_o - B)$ ; and (b) the nucleated condensation model,  $K = 1/(A_o - B)$  using  $A_o = 5.8$ . The values of  $\Delta \bar{V}$  were determined from the slopes of the least-squares lines for each experimental temperature, as described in the text. At complete depolymerization, for the nucleated condensation model,  $K = 1/A_o = 0.172$ .

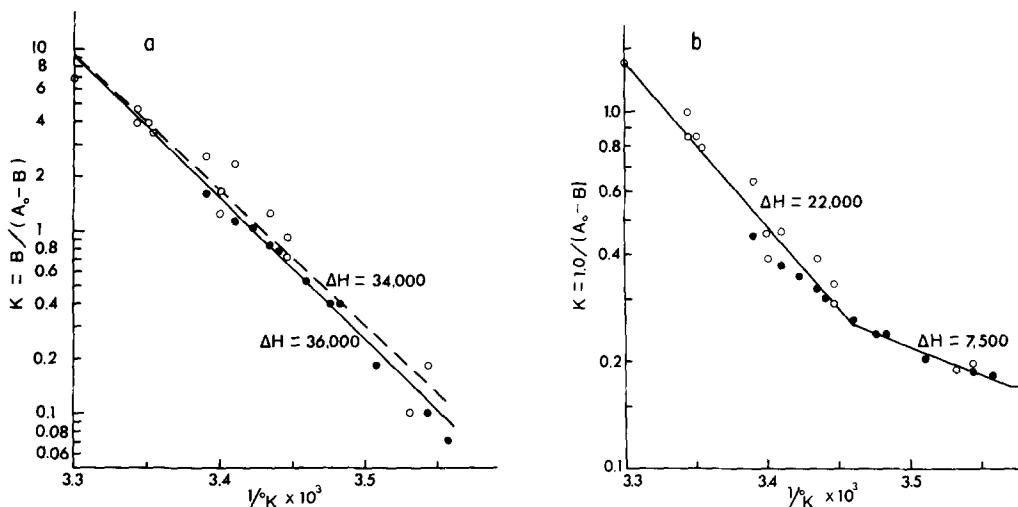


FIGURE 8 Dependence of the equilibrium constant on reciprocal temperature (van't Hoff analysis). The equilibrium constants were found for Inoué's data (open circles) (20), and for data from the present experiments for temperatures  $\leq 22^\circ\text{C}$  (solid circles), with  $A_o = 5.8$ : (a) according to the simple equilibrium model,  $K = (B)/(A_o - B)$ ; and (b) according to the nucleated condensation model,  $K = 1/(A_o - B)$ . The values of  $\Delta H$  were determined from the slopes of the least-squares lines as described in the text.

tion mechanism (37), such a mechanism has not been connected in any way, as yet, with the assembly of microtubules.

## DISCUSSION

The changes in equilibrium spindle BR with pressure agree remarkably well with the changes

predicted from Inoué's simple equilibrium model within the experimentally defined times for pressure equilibrium and over the temperature range  $0^\circ$ – $22^\circ\text{C}$ . Although this result was expected from the previously demonstrated predictability of the model for the dependence of spindle BR on temperature (6, 12, 20, 21, 25, 50, 55), it is not



TABLE I  
Comparison of the Thermodynamic Parameters Found for In Vivo Spindle Microtubule Polymerization with Those of Several In Vitro Polymerization Systems

Polymerizing System	$\Delta H$	$\Delta S$	$\Delta \bar{V}$	Reference
	kcal/mol	eu	ml/mol	
Spindles				
<i>Chaetopterus pergamentaceus</i>				
Simple equilibrium model	36	124	400	*
Nucleated condensation model	7.5-22.0	—	90†	*
Linear condensation model	56	—	525	*
<i>Pectinaria gouldii</i>				
in H <sub>2</sub> O	82.2	286	—	(6)
in D <sub>2</sub> O	59.0	208	—	(6)
<i>Pisaster ochraceus</i>				
in H <sub>2</sub> O	58.9	210	—	(50)
in D <sub>2</sub> O	29.6	106	—	(50)
<i>Tilia americana</i>				
	33.8	123	—	(11)
<i>Strongylocentrotus droebachiensis</i>				
grown at 0°C	64.5	233	—	(55)
grown at 8°C	54.9	197	—	(55)
In vitro systems				
G-ATP actin	10-15	—	—	(1)
	—	—	391	(19)
G-ADP actin	40	119	—	(16)
	—	—	391	(19)
TMV protein	206	739	—	(52)
	—	—	357	(56)
Bacterial flagellin	—	—	150-300	(15)
Brain tubulin	21	96	—	(13)
	—	—	90	(footnote 1)

\* This report.

† Except under circumstances explained in the text.

easily explained. Inoué's simple equilibrium model is an empirical model, and when it was proposed it was not intended to specify any particular molecular mechanism for polymerization of microtubules. On the other hand, a nucleated condensation model, now generally agreed to represent the mechanism of microtubule polymerization in vitro (13, 41)<sup>1</sup>, can be made to fit the pressure and temperature data of the present experiments in vivo while retaining Inoué's assumptions that spindle BR is proportional to degree of spindle microtubule polymerization and that there is a pool of tubulin subunits from which the spindle microtubules are polymerized. The similarity between the thermodynamic parameters found here for the association of spindle microtubules and those found recently for the polymerization of brain microtubules in vitro (13)<sup>1</sup> confirms that spindle microtubules are endothermically self as-

sembled from a pool of tubulin subunits. The kinetics of assembly and disassembly of spindle microtubules and brain microtubules in vitro induced by shifts in pressure and temperature are also remarkably alike (13, 23, 38, 41).<sup>1</sup>

The decrease in spindle BR and size with temperatures above 23°C was unexpected from Inoué's data (20), but it may be related to differences in the habitats of the two populations of experimental animals. The *Chaetopterus* used by Inoué were collected from shallow waters near the shore where temperatures of 30°C or higher are likely to occur, whereas *Chaetopterus* used in the present experiments were collected from water 30 ft deep where temperatures higher than 22°C would rarely, if ever, occur (personal communication from John Valois, Marine Biological Laboratories, Supply Dept., Woods Hole, Mass.). The close correspondence of the present data below

22°C to Inoué's original data suggests that the basic spindle assembly mechanism is the same for both populations; an additional mechanism appears to be responsible for the decrease in spindle BR at higher temperatures. Progressive thermal denaturation of the unpolymerized tubulin subunits that reduces the tubulin pool,  $A_0$ , with increasing temperature above 22°C appears to be the most likely mechanism (14, 15).

The values of  $\Delta H$  and  $\Delta S$  determined from the present experiments are similar to the values found for the assembly of meiotic and mitotic metaphase spindles in a variety of cell types (Table I). Slight differences in experimental technique could cause the variations in values of  $\Delta H$  and  $\Delta S$  among the cell types, but slight differences in the physiological condition of the cell interiors are probably responsible. For example, reductions of only 0.1 U in ionic strength or increases of 0.6 U in pH can induce complete disassembly of TMV protein (32).

Which is more likely: that depolymerization is mediated by the effects of pressure on physiological factors; or that increased pressure depolymerizes microtubules directly? The former possibility can be discounted by evidence (28) that moderate pressure enhances ionization and decreases pH, such effects being expected to enhance polymerization, not depolymerization of microtubules (29). Also, pressures less than 5,000 psi have a negligible effect on rates of cellular metabolism (36, 62). On the other hand, pressure could affect the spindle microtubules directly through the large molar volume increase associated with polymerization,  $\Delta V \approx 100$ –500 ml/mol. At the experimental temperatures the large positive  $\Delta V$  and low  $\Delta G^\ddagger$  readily account for the spindle microtubules being easily depolymerized by pressure.

The estimated magnitudes of  $\Delta V$  are also comparable to the volume changes associated with in vitro polymerization of purified brain microtubules (41)<sup>1</sup> and other protein aggregates that are self-assembled from identical subunits (Table I). Since polymerization for all these proteins is endothermic, the necessary decrease in free energy must be derived from a large increase in entropy, even though one would expect the aggregation of subunits into a much larger structure to involve a decrease in entropy. As a number of hydrophobic or ionic residues are transferred into intermolecular bonds while polymerization proceeds, the release and randomization of constricted bound water could produce the large positive entropy as well as the large molar volume increase of polym-

erization (37). It has been estimated from measurements of buoyant density that about 96 mol of water per mole of polymerizing unit (mol wt  $\approx$  52,000) are released during polymerization of TMV protein (56). The transferral of one nonpolar group from a polar to a nonpolar environment is characterized by an estimated  $\Delta V \approx 20$  ml/mol (31). On this basis, 5–25 hydrophobic residues per tubulin subunit would need to be transferred to a nonionic environment to account for the 100–500 ml/mol volume change in the assembly of spindle microtubules. The tubulin monomer (mol wt  $\approx$  56,000) does have a high percentage of hydrophobic residues, approximately 37% (derived from reference 53), which is typical of proteins for which hydrophobic bonding plays a major role in their aggregation (59).

Although the thermodynamic characteristics of the spindle assembly process have now been determined, the identity of cellular factors that control the normal assembly and disassembly of the spindle during mitosis and the actual molecular mechanisms of spindle microtubule polymerization still remain largely a mystery.

An important assumption for both the simple equilibrium model and nucleated condensation model is that the degree of spindle microtubule polymerization is limited by the availability of a finite and fixed number of tubulin subunits. As mentioned previously, there is a presynthesized pool of tubulin in the cell. Because only 10–20% of the total tubulin content of sea urchin oocytes can be immediately polymerized into spindle microtubules (7, 43), there may be different types of tubulins (2), or a flexible physical or chemical partitioning of the tubulin within the cell (43, 44, 54, 60). The spindle's adaptation to long-term pressurization, similar to that of the axonemal microtubules of the protozoan *Echinospiraerium* (58), could be explained by an activating or partitioning mechanism that is induced to mobilize tubulin for spindle microtubule polymerization by the long-term pressurization.

Although the simple equilibrium model describes both the pressure and the temperature data better than does the nucleated condensation model, the differences are not large and it is impossible to conclude that either model is the "correct" one. The better fit of the simple equilibrium model to the data here and elsewhere (12, 55) may reflect the ability of microtubules to exchange subunits along their lengths (4, 8, 25, 55, 60), but it does not necessarily imply the physically unlikely

situation of a first-order polymerization-depolymerization mechanism of spindle microtubule assembly.

That the same value of  $\Delta V$ , 90 ml/mol, was estimated from both the spindle BR data and data for the assembly of neural microtubules in vitro<sup>1</sup> supports the possibility that spindle microtubules are assembled by a nucleated condensation mechanism. The values of  $\Delta H$  and  $\Delta V$  determined here are the enthalpy and volume changes per polymerizing unit, not per tubulin dimer. Hence, the apparent  $\Delta H$  and  $\Delta V$  could change as a result of a change in the association of the polymerizing unit (e.g., dimer to hexamer) without a change in the actual value of  $\Delta V$  per dimer. Even for the in vitro polymerization of microtubules, the exact nature of the polymerizing subunit or subunits is not yet known (9, 33, 41, 44, 61). Possibly, above 16°C at atmospheric pressure and below 650 psi at 22°C, the size of the polymerizing subunit in the assembly of the *Chaetopterus* spindle triples, thus producing the apparent threefold increase in the values of  $\Delta H$  and  $\Delta V$ . On the other hand, because microtubules in the spindle appear to have different stabilities (continuous and astral microtubules, for instance, are more easily depolymerized than kinetochore microtubules) (47), more than one equilibrium constant may actually govern the spindle assembly reaction. Two classes of microtubules having different stabilities would account for the biphasic character of the data as analyzed by the nucleated condensation model in Figs. 7 b and 8 b as well as the biphasic nature of the kinetic changes in the BR of *Chaetopterus* spindles induced by sudden pressure changes as reported earlier (47).

Thus far, the tendency has been to treat the polymerization of spindle microtubules as if it were occurring in a test tube solution of tubulin with the appropriate distribution of nucleating sites. Increasing evidence, however, requires us to consider the great oversimplification of this assumption. For instance, the various types of microtubules in the spindle (i.e. chromosomal, continuous, astral) not only have different stabilities, but they shorten and elongate at different times during mitosis in spite of their close proximity (3, 24, 48). That polymerization is not homogeneous within the spindle is demonstrated by the considerable fluctuations in the BR of individual chromosomal fibers, particularly during prometaphase (21, 34). Areas of reduced chromosomal fiber BR produced by UV microbeam irradiation (10) have

been shown to move poleward during metaphase or anaphase at a velocity similar to that of chromosomes during anaphase. When a multipolar spindle reforms after the release of high pressure, its BR indicates that more tubulin has been polymerized into spindle microtubules than would have been polymerized into a bipolar spindle under the same circumstances (46).

Although the results of the present and previous experiments have not permitted the specific polymerization mechanism for assembling spindle fiber microtubules to be defined, the results here do emphasize that the thermodynamic character of polymerization within the living mitotic spindle is similar to polymerization of microtubules in vitro. The spindle does behave as though it was in an equilibrium with a pool of dissociated subunits, but the actual method by which the subunits become associated is not clear. Because cytoplasmic conditions within the spindle region are not likely to be as homogeneous as conditions in the test tube, future efforts are needed to elucidate the function of nucleating and orienting centers within the spindle, especially their possible roles in controlling the size of the spindle's tubulin pool, in anchoring microtubules within the spindle, and regulating local and selective polymerization and depolymerization of the microtubules.

I wish to thank Dr. S. Inoué for his valuable advice, for providing laboratory facilities and equipment, and for his critical reading of the manuscript. I would also like to express my appreciation for the thoughtful discussions and suggestions of Drs. G. Ellis, R. E. Stephens, J. Fuseler, and D. Begg, as well as Drs. G. G. Borisy and K. Johnson concerning the mechanism of spindle assembly.

Portions of this work were submitted in partial fulfillment of the requirements for the Doctor of Philosophy degree at the University of Pennsylvania.

This work was carried out under grant CA10171 and training grant GM00606 from the National Institutes of Health and grant GB31739X from the National Science Foundation.

Received for publication 29 March 1974, and in revised form 26 March 1975.

## APPENDIX

The equilibrium constant  $K$  and the standard free energy change of a reaction  $\Delta G^{\circ}$  are related by:

$$-RT(\ln K) = \Delta G^{\circ}.$$

The behavior of the equilibrium constant with pressure

and temperature can be written (27):

$$K(T,P) = \exp \left[ -(\Delta G_1^0/RT) - \int_{P=1}^P \frac{d\Delta G^0}{dP} dP \right],$$

Where  $\Delta G_1^0 = \Delta H - T\Delta S$  with  $\Delta G_1^0$ ,  $\Delta H$ , and  $\Delta S$ , respectively, the changes in standard free energy, enthalpy, and entropy at one atmosphere pressure and temperature  $T$ . The pressure dependence of  $\Delta G^0$  is given by  $d\Delta G^0/dP = \Delta \bar{V}$  where  $\Delta \bar{V}$  is the difference in the molar volumes between the final products and the initial reactants. The pressure coefficient of  $\Delta \bar{V}$  for condensed systems is small for pressure up to 5,000 psi (18). After integration in the above equation:

$$K(T,P) = \exp [-(\Delta G_1/RT) - (P - 14.7)\Delta V/RT],$$

where pressure is measured in units of psi and temperature in degrees Kelvin.

## REFERENCES

1. ASAKURA, S., M. KASAI, and F. OOSAWA. 1960. The effect of temperature on the equilibrium state of actin solutions. *J. Polym. Sci. Part D Macromol. Rev.* **44**:35-49.
2. BEHNKE, O., and A. FORER. 1967. Evidence for four classes of microtubules in individual cells. *J. Cell Sci.* **2**:169-192.
3. BRINKLEY, B. R., and J. CARTWRIGHT, JR. 1971. Ultrastructural analysis of mitotic spindle elongation in mammalian cells in vitro. Direct microtubule counts. *J. Cell Biol.* **50**:416-431.
4. BURKHOLDER, G. D., T. A. OKADA, and D. E. COMINGS. 1972. Whole mount electron microscopy of metaphase I chromosomes and microtubules from mouse oocytes. *Exp. Cell Res.* **75**:497-511.
5. CANDE, W. Z., J. SNYDER, D. SMITH, K. SUMMERS, and J. R. MCINTOSH. 1974. A functional mitotic spindle prepared from mammalian cells in culture. *Proc. Natl. Acad. Sci. U. S. A.* **71**:1559-1563.
6. CAROLAN, R. M., H. SATO, and S. INOUÉ. 1966. Further observations on the thermodynamics of the living mitotic spindle. *Bull. Bull. (Woods Hole)*. **131**:385. (Abstr.).
7. COHEN, W. D., and L. I. REBHUN. 1970. An estimate of the amount of microtubule protein in the isolated mitotic apparatus. *J. Cell Sci.* **6**:159-176.
8. DIETZ, R. 1972. Die Assembly-Hypothese der Chromosomenbewegung und die Veränderungen der Spindellänge während der Anaphase I in Spermatozyten von *Pales ferruginea* (Tipulidae, Diptera). *Chromosoma (Berl.)*. **38**:11-76.
9. ERICKSON, H. P. 1974. Assembly of microtubules from preformed ring-shaped protofilaments and 6S tubulin. *J. Supramol. Struct.* **2**:393-411.
10. FORER, A. 1965. Local reduction in spindle fiber birefringence in living *Nephrotoma suturalis* (Loew) spermatocytes induced by ultraviolet microbeam irradiation. *J. Cell Biol.* **25** (1, Pt. 2):95-117. (Mitosis suppl.).
11. FUSELER, J. W. 1972. Unusual aspects of chromosome movement and phragmoplast formation in *Tilia americana*. *Biol. Bull. (Woods Hole)*. **143**:474. (Abstr.).
12. FUSELER, J. W. 1973. The effect of temperature on chromosome movement and the assembly-disassembly process of birefringent spindle fibers in actively dividing plant and animal cells. Ph.D. Thesis. University of Pennsylvania, Philadelphia, Pa. University Microfilms, Ann Arbor, Mich.
13. GASKIN, F., C. R. CANTOR, and M. L. SHELANSKI. 1974. Turbidometric studies of the in vitro assembly and disassembly of porcine microtubules. *J. Mol. Biol.* **89**:737-758.
14. GERBER, B. R., S. ASAKURA, and F. OOSAWA. 1973. Effect of temperature on the in vitro assembly of bacterial flagella. *J. Mol. Biol.* **74**:467-487.
15. GERBER, B. R., and H. NOGUCHI. 1967. Volume change associated with the G-F transformation of flagellin. *J. Mol. Biol.* **26**:197-210.
16. GRANT, R. J. 1965. Reversibility of G-actin-ADP polymerization—physical chemical organization. Ph.D. Thesis. Columbia University, New York.
17. GOLDMAN, R. D., and L. I. REBHUN. 1969. The structure and some properties of the isolated mitotic apparatus. *J. Cell Sci.* **4**:179-209.
18. HAMANN, S. D. 1963. Chemical equilibria in condensed systems. In *High Pressure Physics and Chemistry*. R. S. Bradley, editor. Academic Press, Inc., London. 131-162.
19. IKKAI, R., T. OOI, and H. NOGUCHI. 1966. Actin: volume change on transformation of G-form to F-form. *Science (Wash. D.C.)*. **152**:1756-1757.
20. INOUÉ, S. 1959. Motility of cilia and the mechanism of mitosis. *Rev. Mod. Phys.* **31**:402-408.
21. INOUÉ, S. 1964. Organization and function of the mitotic spindle. In *Primitive Motile Systems in Cell Biology*. R. D. Allen and N. Kamiya, editors. Academic Press, Inc., New York. 549-594.
22. INOUÉ, S., G. G. BORISY, and D. P. KIEHART. 1974. Growth and lability of *Chaetopterus* oocyte mitotic spindles isolated in presence of porcine brain tubulin. *J. Cell Biol.* **62**:175-184.
23. INOUÉ, S., J. FUSELER, E. D. SALMON, and G. W. ELLIS. 1975. Functional organization of mitotic microtubules—physical chemistry of the in vivo equilibrium system. *Biophys. J.* In press.
24. INOUÉ, S., and H. RITTER. 1975. Dynamics of mitotic spindle organization and function. In *Molecules and Cell Movement*. R. E. Stephens and S. Inoué, editors. Raven Press, New York. In press.
25. INOUÉ, S., and H. SATO. 1967. Cell motility by labile association of molecules. The nature of mitotic spindle fibers and their role in chromosome movement. *J. Gen. Physiol.* **50**:259-292.
26. JENSEN, C., and A. BAJER. 1973. Spindle dynamics

- and arrangement of microtubules. *Chromosoma (Berl.)*. **44**:73-89.
27. JOHNSON, F. H., and H. EYRING. 1970. The kinetic basis of pressure effects in biology and chemistry. In *High Pressure Effects on Cellular Processes*. A. M. Zimmerman, editor. Academic Press, Inc., New York. 1-44.
  28. JOHNSON, F. H., H. EYRING, and M. J. POLISSAR. 1954. *The Kinetic Basis of Molecular Biology*. John Wiley & Sons, Inc., New York.
  29. KANE, R. E. 1965. The mitotic apparatus. Physical-chemical factors controlling stability. *J. Cell Biol.* **25**:137-144.
  30. KASAI, M. 1969. Thermodynamical aspect of G-F transformations of actin. *Biochim. Biophys. Acta.* **180**:399-409.
  31. KAUZMAN, W. 1959. Factors in interpretation of protein denaturation. *Adv. Protein Chem.* **1**:1-58.
  32. KHALIL, M. T. M., and M. A. LAUFFER. 1967. Polymerization-depolymerization of tobacco mosaic virus protein. X. Effect of D<sub>2</sub>O. *Biochemistry.* **6**:2474-2480.
  33. KIRSCHNER, M. W., and R. C. WILLIAMS. 1975. The mechanism of microtubule assembly in vitro. *J. Supramol. Struct.* **2**:412-428.
  34. LAFOUNTAIN, J. R., JR. 1972. Changes in the patterns of birefringence and filament deployment in the mitotic spindle of *Nephrotoma suturalis* during first meiotic division. *Protoplasma.* **75**:1-17.
  35. LAFOUNTAIN, J. R., JR. 1974. Birefringence and fine structure of spindles in spermatocytes of *Nephrotoma suturalis* at metaphase at first meiotic division. *J. Ultrastruct. Res.* **46**:268-278.
  36. LANDAU, J. V. 1970. Hydrostatic pressure on the biosynthesis of macromolecules. In *High Pressure Effects on Cellular Processes*. A. M. Zimmerman, editor. Academic Press, Inc., New York. 45-70.
  37. LAUFFER, M. A. 1971. Tobacco mosaic virus and its protein. In *Biological Macromolecules*. S. N. Timasheff and G. D. Fasman, editors. Marcel Dekker, Inc., New York. 5:149-200.
  38. LEE, Y. C., F. E. SAMSON, JR., L. L. HOUSTON, and R. H. HIMES. 1974. The in vitro polymerization of tubulin from beef brain. *J. Neurobiol.* **5**:317-330.
  39. MALAWISTA, S. E., H. SATO, and K. G. BENSCH. 1968. Vinblastin and griseofulvin reversibly disrupt the living mitotic spindle. *Science (Wash. D.C.)*. **160**:770-772.
  40. NICKLAS, R. B. 1971. Mitosis. In *Advances in Cell Biology*, D. M. Prescott, L. Goldstein, and E. H. Conkey, editors. Appleton-Century-Crofts, Inc., New York. 2:225-298.
  41. OLMSTED, J. B., J. M. MARCUM, K. A. JOHNSON, C. ALLEN, and G. G. BORISY. 1974. Microtubule assembly: some possible regulatory mechanisms. *J. Supramol. Struct.* **2**:429-450.
  42. OOSAWA, R., and M. KASAI. 1971. Actin. In *Biological Macromolecules*. S. N. Timasheff and G. D. Fasman, editors. Marcel Dekker, Inc., New York. 5: 261-322.
  43. RAFF, R. A., G. GREENHOUSE, K. W. GROSS, and P. R. GROSS. 1971. Synthesis and storage of microtubule proteins by sea urchin embryos. *J. Cell Biol.* **50**:516-527.
  44. REBHUN, L. I., M. MELLON, D. JEMIOLO, J. NATH, and N. IVY. 1974. Regulation of size and birefringence of the in vivo mitotic apparatus. *J. Supramol. Struct.* **2**:466-485.
  45. REBHUN, L. I., and G. SANDER. 1967. Ultrastructure and birefringence of the isolated mitotic apparatus of marine eggs. *J. Cell Biol.* **34**:859-883.
  46. SALMON, E. D. 1973. The effects of hydrostatic pressure on the structure and function of the mitotic spindle: an in vivo analysis with a newly developed pressure chamber. Ph.D. Thesis. University of Pennsylvania, Philadelphia, Pa. University Microfilms, Ann Arbor, Mich.
  47. SALMON, E. D. 1975 a. Pressure-induced depolymerization of spindle microtubules. I. Changes in birefringence and spindle length. *J. Cell Biol.* **65**:603-614.
  48. SALMON, E. D. 1975 b. Spindle microtubules: thermodynamics of in vivo assembly and role in chromosome movement. *Ann. N. Y. Acad. Sci.* **253**:383-406.
  49. SALMON, E. D., and G. W. ELLIS. 1975. A new miniature hydrostatic pressure chamber for microscopy. *J. Cell Biol.* **65**:587-602.
  50. SATO, H., and J. BRYAN. 1968. Thermodynamics of molecular association in the mitotic spindle. *J. Cell Biol.* **39** (2, Pt. 2): 118 a. (Abstr.).
  51. SATO, H., S. INOUÉ, and G. W. ELLIS. 1971. The microtubular origin of spindle birefringence: experimental verification of Wiener's equation. Proceedings of the 11th Annual Meeting of the American Society of Cell Biology. (Abstr.).
  52. SMITH, C. E., and M. A. LAUFFER. 1967. Polymerization-depolymerization of tobacco mosaic virus protein. VIII. Light-scattering studies. *Biochemistry.* **6**:2457-2465.
  53. STEPHENS, R. E. 1971. Microtubules. In *Biological Macromolecules*. S. N. Timasheff and G. D. Fasman, editors. Marcel Dekker, Inc., New York. 5:355-391.
  54. STEPHENS, R. E. 1972. Studies on the development of the sea urchin *Strongylocentrotus droebachiensis*. II. Regulation of mitotic spindle equilibrium by environmental temperature. *Biol. Bull. (Woods Hole)*. **142**:145-159.
  55. STEPHENS, R. E. 1973. A thermodynamic analysis of mitotic spindle equilibrium at active metaphase. *J. Cell Biol.* **57**:133-147.
  56. STEVENS, C. L., and M. A. LAUFFER. 1965. Polymerization-depolymerization of tobacco mosaic virus protein. IV. The role of water. *Biochemistry.* **4**:31-37.

57. TAYLOR, E. W. 1963. Relation of protein synthesis to the division cycle in mammalian cell cultures. *J. Cell Biol.* **19**:1-18.
58. TILNEY, L., Y. HIRAMOTO, and D. MARSLAND. 1966. Studies on the microtubules in Heliozoa. III. A pressure analysis of the role of these structures in the formation and maintenance of the axopodia of *Actinosphaerium nucleofilum* (Barrett). *J. Cell Biol.* **29**:77-95.
59. VAN HOLDE, K. E. 1966. The molecular architecture of multichain proteins. In *Molecular Architecture in Cell Physiology*. T. Hayashi and A. G. Szent-Gyorgi, editors. Prentice-Hall, Inc., Englewood Cliffs, N. J. 81-96.
60. WEISENBERG, R. C. 1972. Changes in the organization of tubulin during mitosis in the eggs of the surf clam *Spisula solidissima*. *J. Cell Biol.* **54**:266-278.
61. WEISENBERG, R. C. 1974. The role of ring aggregates and other structures in the assembly of microtubules. *J. Supramol. Struct.* **2**:451-465.
62. ZIMMERMAN, A. M. 1970. High pressure studies on synthesis in marine eggs. In *High Pressure Effects on Cellular Processes*. A. M. Zimmerman, editor. Academic Press, Inc., New York. 235-259.